Polym. Bull. (2012) 68:961–972
DOI 10.1007/s00289-011-0589-6

ORIGINAL PAPER

Synthesis and characterization of sol–gel derived PVA-titanium dioxide (TiO_2) nanocomposite

Archana Maurya · Pratima Chauhan

Received: 10 June 2010 / Revised: 7 July 2011 / Accepted: 21 July 2011 /
Published online: 31 July 2011

Abstract Novel PVA/TiO_2 polymer nanocomposites have been prepared at low temperature via sol–gel route. XRD analysis showed the particles to be elongated along *a*- and *b*-direction but contracted along *c*-direction. PVA-assisted TiO_2 nanocomposite samples dried at a temperature of 35 °C were found to have ~12 nm particle size. It was found that the composite nanoparticles had an increased degree of crystallinity in comparison to pure TiO_2 dried at 80 °C. TEM analysis depicted the formation of highly dense nanorods (and prism)-like structure of increasing length and diameter depending on PVA concentration. Our studies revealed that by increasing the concentration of PVA in TiO_2 the band gap was lowered from 3.55 to 1.65 eV. The photoluminescence studies showed that emission shifts towards higher wavelength (417–457 nm) accompanied by a reduction in impurity centres with increasing concentration of PVA in TiO_2.

Keywords Polymeric-matrix composites (PMCs) · Sol–gel methods · Structural characterization · Optical characterization

Introduction

Recently, organic–inorganic hybrid materials have been extensively investigated. One obtains new kind of composite materials with synergetic or complementary behaviours, which can be used in electronic or nanoelectronic devices [1–4]. Hybrid

A. Maurya (✉) · P. Chauhan
UGC Centre of Advanced Studies, Department of Physics, University of Allahabad, Allahabad 211002, India
e-mail: v.arch17@gmail.com

P. Chauhan
e-mail: mangu167@yahoo.co.in

materials have become the main focus in the material science because of their specific electronic properties, which can be tailored via synthetic organic chemistry.

TiO_2 is an important functional material, widely used for various applications including photo-electrochemical activity [5], solar energy conversion [6], photocatalysis [7], UV detectors, ultrasonic sensors, etc. Environmental compatibility, non-toxicity and low price are some practical advantages of TiO_2. As a catalyst and/or catalyst support, it is employed in the process of photo-degradation. It is one of the typical n-type semiconductor, while polyvinyl alcohol (PVA) is one of the typical conducting polymer. Because PVA has excellent film forming, emulsifying and adhesive properties, it has potential application in many fields such as in the food industries as a binding and coating agent, in the immobilization of activated sludge[8], in controlled release of drug [9], in electrochemical cells [10], etc. Among the entire conducting polymers, PVA has a special status due to the presence of reactive –OH groups in polymer chain. Tetragonal structure of titanium dioxide (TiO_2) and that of polymer PVA are shown below in Fig. 1. TiO_2/polymer nanocomposites show a special property such as capability of intense absorbing UV radiation as well as excellent transparency for the visible light. Such organic–inorganic hybrid composite membranes have potential applications in optical and cosmetic fields as well as food packaging materials [12].Although a large number of studies on composite materials of polyvinyl alcohol and TiO_2 have been reported, most of the researches on these polymers are still focusing on the preparation of materials and morphology characterization, such as size and shape of the oxide particles, degree of dispersion, kind of interaction and interface between organic and inorganic phase, and so on. Yang [11] have prepared PVA/TiO_2 composite by solution casting method and characterized it for the application of direct methanol fuel cell. Sairam et al. [12] have prepared PVA/TiO_2 mixed matrix membranes by incorporating nano-sized titanium dioxide and titanium dioxide surface modified with polyaniline into PVA and crosslinked with glutaraldehyde for pervaporation separation of water–isopropanol mixtures. Recently a controlled crystallization of titanium dioxide particles from peroxytitanic acid in the presence of PVA has been reported by Wang et al. [13]. But their result appears to be highly dependent on the pH condition. A very few reports touched upon the PVA assisted change in structural and optical property of TiO_2.

In this study, efforts have been made to enhance the structural and optical stability of TiO_2 with the help of polyvinyl alcohol without the use of any pH

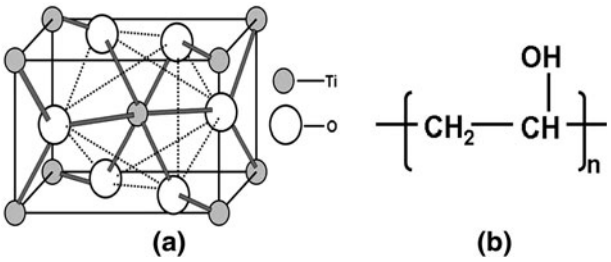

Fig. 1 **a** Tetragonal unit cell structure of rutile titanium dioxide (TiO_2): the *grey* and *white spheres* represent Ti and O atoms, and **b** that of polymer polyvinyl alcohol (PVA)

adjusting precursor. A strong effect on the nanostructured feature and optical properties of TiO_2 has been observed when it was mixed with PVA. The correlation between polyvinyl alcohol and TiO_2 is also discussed by UV–Vis and PL spectra. By the use of organic–inorganic approach, we have tried to improve the structural and optical performance of TiO_2.

Experimental section

Materials

Titanium (IV) chloride (anhydrous), MW = 189.71, density (d_4^{20}) = 1.729–1.730 and Min. Assay (Argentometric) of 99% and PVA (Merck), M.W. = 145,000 and degree of hydrolysis $\geq$ 98 were used as starting materials. Ethanol (Merck), density (d 20/20 °C) = 0.790–0.793 and purity of 99.9% was commercially available. Double distilled water was used for all studies.

Preparation of pure TiO_2

Titanium tetrachloride was used as the starting material to prepare pure TiO_2 by sol–gel method. 3 mL of $TiCl_4$ was added in drops to 100 mL of double distilled chilled water (0 °C) at constant stirring to prepare TiO_2 nanoparticles. A colourless solution was obtained which was further stirred for 2 h in order to complete the reaction and after leaving the solution for 24 h we obtained a white precipitate. The white precipitate has been washed with ethanol and double distilled water and then dried it at a temperature of 80 °C.

Preparation of PVA/TiO_2 nanocomposites

PVA polymer matrix (2 and 4 wt%, respectively) was dispersed in 100 mL of double distilled water and stirred for 2 h at temperature of 80 °C until a viscous transparent solution was obtained. After that the solution was cooled at a temperature of 0 °C and then 3 mL of $TiCl_4$ was added dropwised to the PVA solution and stirred for 2 h in order to complete the reaction. Thus, formed PVA/TiO_2 composite was isolated by centrifugation and washed with ethanol and double distilled water to remove any by-product. The composite was dried at 35 °C for four hours. We have noticed that the precipitation time increased with increasing PVA concentration (3 days when PVA = 2 wt% and 7 days when PVA = 4 wt%). We have not used any precursor to adjust the pH value of the solution. In all the cases, precipitation occurs at pH less than 1.

Characterization

The structural characterization of the nanoparticles was carried out by analysis of the XRD pattern using a RIGAKU X-ray diffractometer with Cu Kα (1.54 Å) radiation in the 2θ range 20°–60°. Transmission electron microscopy (TEM), high resolution TEM (HRTEM) were performed by using Tecnai 30 G2 S-Twin electron

microscope operating at 300 kV accelerating voltage. The band gaps of the nanoparticles were investigated by optical absorption studies carried out using a UV–Vis spectrophotometer (Lambda 35 Perkin Elmer in the range 200-800 nm). Photoluminescence (PL) studies of the samples have also been carried out using LS 55 Perkin Elmer spectrophotometer with 340 and 375 nm excitation line of xenon discharge lamp.

Result and discussion

The X-ray diffraction measurements were performed to examine the nanostructured feature and crystallinity of the pure TiO_2 and PVA/TiO_2 polymer nanocomposites. Figure 2a and b shows the X-ray diffraction patterns of TiO_2 and PVA, respectively. Whereas, Fig. 2c and d shows the X-ray diffraction patterns of PVA/TiO_2 composite having 2 and 4 wt% of PVA, respectively. It has been observed that XRD patterns for all the samples correspond to a rutile phase of TiO_2. The XRD patterns for the composite samples prepared under the same experimental condition but dried at 35 °C were not so different from those of pure TiO_2 sample except for a slight increase in overall peak intensity. PVA is a well known crystalline polymer, and the diffraction peaks at $2\theta = 19.58°$ and 23.38° correspond to the crystalline phase of PVA in the as prepared nanocomposite samples. Further, diffraction peaks at $2\theta = 27.43°$, 36.09°, 41.15°, 54.31° and 56.41° corresponds to (110), (101), (111), (211) and (220) plane reflection of tetragonal rutile TiO_2 while a peak at 43.80° corresponds to $(2\bar{3}1)$ plane reflection of tetragonal rutile phase of TiO. From the XRD studies, unit cell of the prepared samples was arrived at as tetragonal with lattice parameter $a = b = 4.62$ Å and $c = 2.94$ Å. However, according to JCPDS no. 21-1276 lattice parameters for tetragonal rutile was $a = b = 4.59$ Å and $c = 2.96$ Å. Thus, in our case, an elongation along a- and b-axis whereas a contraction towards c-axis has been observed showing that TiO_2 nanocrystals growth occurs along a- and b-axis direction. The average grain size of all the samples was estimated from X-ray line broadening analysis by the Scherrer equation [14] and it was found that grain size lies between 3–8 nm for pure TiO_2, 5–6 nm for pure PVA, 5–11 nm for PVA/TiO_2 (PVA = 2 wt%) and 7–12 nm for PVA/TiO_2 (PVA = 4 wt%). From XRD curves, it has also been found that the intensity of PVA/TiO_2 diffraction peak got increased. This increase can be attributed due to the interaction between PVA and TiO_2 nanoparticles. Since PVA contains a large number of hydroxyl groups so it can effectively inhibit the aggregation of TiO_2 nanoparticles by the organic surface modification and help to keep the TiO_2 particles well dispersed in the aqueous PVA solution at the nanoscale. Also, from the Gaussian fitting as far as full width half maxima (FWHM) value was considered for the peak at 27.32°, we have found that its value comes out to be 1.3668 for pure TiO_2, 1.1240 for the sample having PVA 2 wt% and 1.0231 for the sample with PVA 4 wt%. It is a well-known fact that a decrease in FWHM value corresponds to the subsequent increase in crystallinity. These results indicate that the crystallinity of PVA/TiO_2 powder becomes much more perfect with the

increasing amount of PVA which resulted from the hydrolysis and polymerization of the precursor. When PVA chain segments are absorbed onto the surfaces of TiO_2 nanoparticles, Ti–OH groups on the surface of TiO_2 nanoparticles will react with the hydroxyl groups linking to the PVA chains. One can thus expect that strong interfacial bond, viz. Ti–O–C (Fig. 3) be formed on the surface of TiO_2 nanoparticles such that surfaces of TiO_2 nanoparticles will be wrapped with the layer of PVA polymer.

Detailed information about the microstructure and morphology has been provided by TEM examination of the sample. The TEM image morphology of the pure TiO_2 and PVA/TiO_2 nanocomposite with PVA = 2 wt% are shown in Fig. 4a and b, respectively. The image showed the formation of nanorods and prism-like structure which are dense and randomly oriented throughout the sample. The samples are highly crystalline in nature as is also confirmed by XRD. The outer diameter of $\sim$4 nm and the longest rod length of $\sim$36 nm were obtained for the case of pure TiO_2 sample. However, an outer diameter of $\sim$20 nm and longest rod length of $\sim$96 nm has been obtained for PVA/TiO_2 nanocomposite sample. The result reveals that adding of PVA in TiO_2 increases the rod width and length. Further details of the structure can be resolved by considering higher magnification HRTEM image of the samples. Figure 5a and b represents the high resolution TEM (HRTEM) image of the same samples. The observed lattice spacing of 0.34 nm corresponds to the (110) plane of rutile TiO_2 showing that the wall of the nanotubes grows along (110) plane for both the samples.

Figure 6 shows the optical absorption (α) feature for the as prepared four samples. As can be seen from the figure, the absorption for pure TiO_2 occurs at $\sim$348 nm ($E_{g(348)} = 3.55$ eV) while pure PVA solution exhibit absorption nearly at

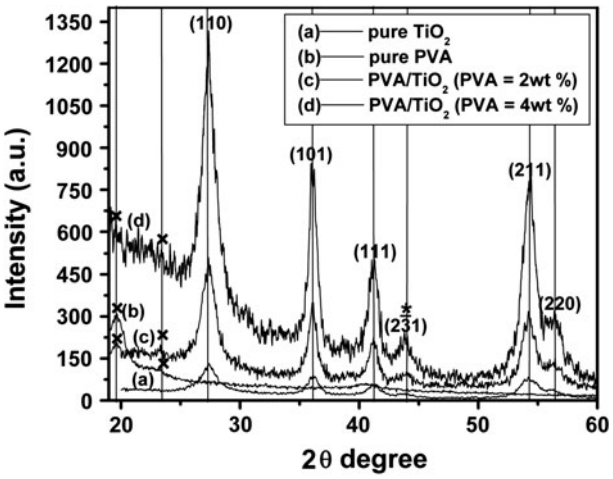

Fig. 2 Powder XRD patterns of: (*a*) pure TiO_2, (*b*) pure PVA, (*c*) PVA/TiO_2 (2 wt%) nanocomposite, and (*d*) PVA/TiO_2 (4 wt%) nanocomposite. Planes (hkl) corresponding to the reflections of rutile phase are marked in the diffraction pattern. Additional phases due to PVA and TiO are marked with *cross* and *asterisk*, respectively

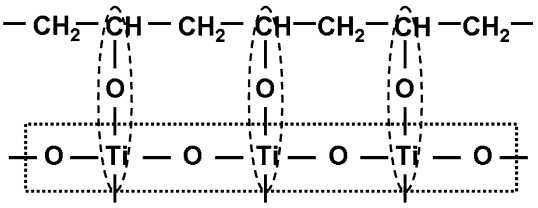

Fig. 3 Surface structure scheme of PVA/TiO_2 nanoparticle

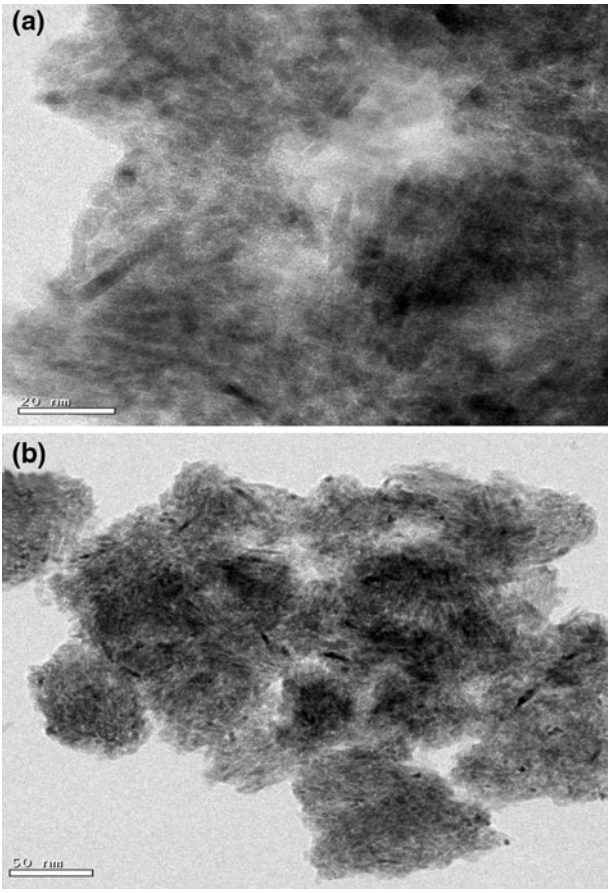

Fig. 4 Transmission electron micrograph (TEM) of the **a** pure TiO_2 sample and **b** PVA/TiO_2 nanocomposite sample with PVA (2 wt%)

$\sim$373 nm ($E_{g(373)} = 3.31$ eV) in the selected region. However, samples corresponding to PVA (2 and 4 wt%) showed absorption edges at about $\sim$690 ($E_{g(690)} = 1.79$ eV) and $\sim$749 nm ($E_{g(749)} = 1.65$ eV), respectively. Thus, it follows from the absorption results that for pure TiO_2 the absorption edge blue shifted for more than 61 nm corresponding to bulk TiO_2($E_{g(409)} = 3.02$ eV). On the other hand, if considering PVA/TiO_2 nanocomposite samples, the case seemed to be

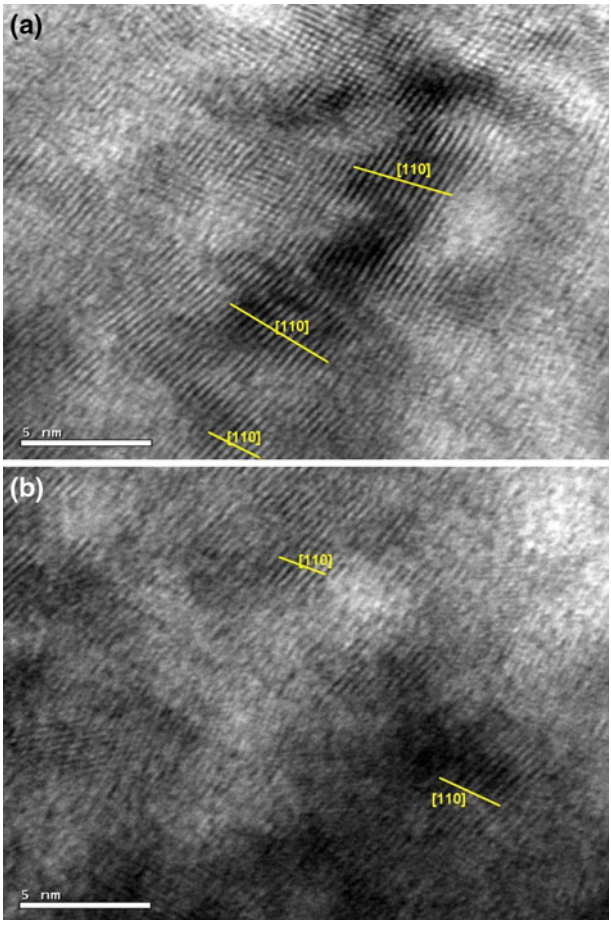

Fig. 5 HRTEM image of **a** pure TiO_2, and **b** PVA/TiO_2 nanocomposite with PVA (2 wt%)

completely different to that of pure TiO_2. For such a case, a red shift in absorption edges rather than blue shift is observed. Since in the UV–Vis absorption spectra, the absorption edge provides information about the index of particle size, i.e., smaller particles have larger band gaps and absorbs at shorter wavelength, a blue shift towards higher band gap attribute a smaller particle size, whereas a red shift corresponds to comparatively a larger particle size in the as prepared composite samples.

About the nature of the band gap for TiO_2 (direct or indirect transition), Meng et al. [15] and Madhu et al. [16] showed that the transition for nanophase TiO_2 was direct, but Mardare et al.[17] found that the transition for TiO_2 was indirect. Now, in order to determine the nature of the band gap, either indirect or direct, the following relation is often used [18]:

$$(\alpha hv) = A\,(hv - E_g)^n$$

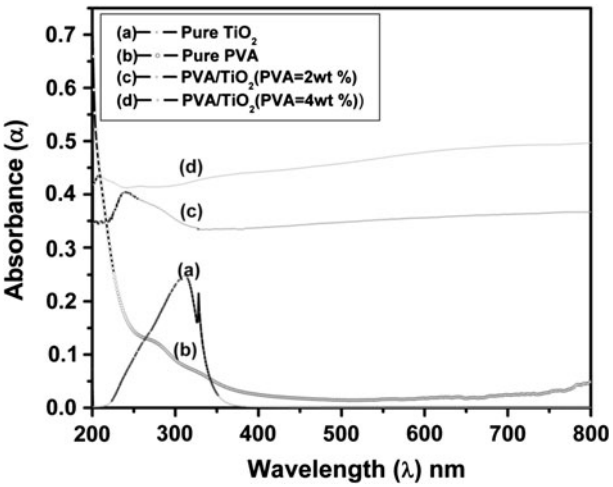

Fig. 6 The UV–Vis absorption spectra of (*a*) pure TiO_2, (*b*) pure PVA, (*c*) PVA/TiO_2 nanocomposite with PVA (2 wt%), and (*d*) PVA/TiO_2 nanocomposite with PVA (4 wt%)

where ($h\nu$) is the photon energy, E_g is the optical band gap, α is absorption coefficient and '*A*' is a constant which does not depend on ($h\nu$). The value of *n* is 2 for indirect transition and ½ for direct transition. Thus, the curve of $(\alpha h\nu)^2$ and $(\alpha h\nu)^{1/2}$ versus photon energy ($h\nu$) determines the nature of the transition. Figures 7 and 8 represent the direct and indirect transition for all the four samples, respectively. A band gap calculation has been done considering these two graphs and the corresponding band gap values are shown in Table 1. From the Table 1, it can be seen that the band gap value goes on decreasing with increasing the amount PVA in TiO_2. A comparison between direct band gap and indirect band gap value reveals that direct transitions dominate over indirect transitions for all the cases. Thus, it may be concluded here that adding of PVA in TiO_2 make the nature of TiO_2 as direct one instead of indirect one. PVA that is usually crystalline in nature resulted from the strong intermolecular interaction among PVA chain through intermolecular hydrogen bonding. Hence, presence of PVA in the reaction mixture modified the nature of bands. Also, in our case a decrease in indirect band gap value implies that the process of non-radiative recombination has become slow with the removal of point defect and grain boundaries. Hence with the help of PVA in TiO_2, we can prevent the excited electrons to reach the recombination places. The confirmation of these results has also been done with the help of PL spectra.

Figure 9 represent the PL spectrum of pure TiO_2 and PVA doped TiO_2 with different amount of PVA and different excitation wavelengths (340 and 375 nm). As can be seen from the graphs that when the samples are excited at a wavelength of 340 nm, which nearly corresponds to the wavelength at maximum absorption, we get PL maxima at a wavelength $\sim$417 nm with some minor peaks at 478 and 521 nm for the case of pure TiO_2 and with PVA (2 wt%) added TiO_2. However, when we further excited the sample at 375 nm, i.e., at excitation energy less than

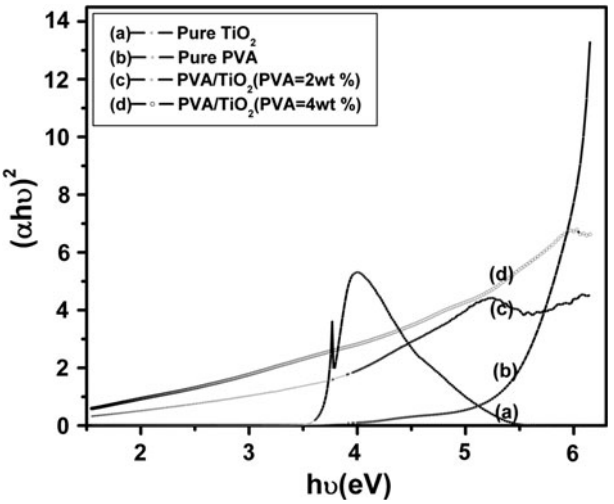

Fig. 7 The UV–Vis absorption spectra of (*a*) pure TiO_2, (*b*) pure PVA, (*c*) PVA/TiO_2 nanocomposite with PVA (2 wt%), and (*d*) PVA/TiO_2 nanocomposite with PVA (4 wt%) for the case of direct allowed transitions

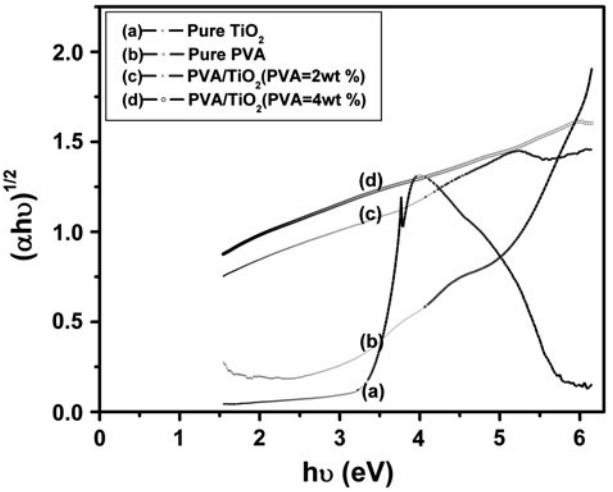

Fig. 8 The UV–Vis absorption spectra of (*a*) pure TiO_2, (*b*) pure PVA, (*c*) PVA/TiO_2 nanocomposite with PVA (2 wt%), and (*d*) PVA/TiO_2 nanocomposite with PVA (4 wt%) for the case of indirect allowed transitions

band gap energy then we get band maxima at 441 nm, which shifts to higher wavelength. However, it can also be seen from the graph that the case is somewhat different when amount of PVA in TiO_2 increased. For this case PL maxima occurs at a wavelength of 457 nm when the sample is excited at $\lambda_{ex} = 340$ nm and further when $\lambda_{ex} = 375$ nm PL peak maxima appears at 488 nm. A shift towards higher wavelength is found when quantity of PVA matrix in TiO_2 increases. We may

Table 1 Band gap analysis of pure TiO_2 and PVA/TiO_2 nanocomposite at different concentration of PVA

Samples	(α) (eV)	$(\alpha hv)^2$ (eV)	$(\alpha hv)^{1/2}$ (eV)
Pure TiO_2	3.55	3.66	3.39
Pure PVA	3.31	5.38	4.31
PVA/TiO_2 (PVA = 2 wt%)	1.79	3.11	2.00
PVA/TiO_2 (PVA = 4 wt%)	1.65	3.17	1.12

conclude that decreasing the excitation energy for PL causes a decrease in energy of the corresponding emission band. It is already noted by other workers that in the nanoclusters of semiconductors associated with defect centres, emission for both bound and free excitons would appear when λ_{ex} is equivalent to E_g and emission for only free excitons in the case $\lambda_{ex} > E_g$ or $< E_g$. Also a strong PL spectrum for TiO_2 indicates that the PL is absolutely related to impurity or oxygen vacancies related centres. Thus, we may conclude here that the peaks at $\lambda_{ex} = E_g$ occur due to emission from both bound and free excitons and the minor peaks in the low energy side are attributed to transition assisted by one, two or three phonon replicas of impurity-related centres. The band for $\lambda_{ex} < E_g$ may be ascribed to the free excitons and the shift with variation of excitation energy is due to the change in nanoclusters size. The particle size has a great effect on the intensities of the PL peak due to interaction of TiO_2 nanoparticles with PVA matrix. In addition, the PL peak became sharper with increasing PVA conc., which is an indication of reduction in impurity related centres in the PVA/TiO_2 nanocomposite samples.

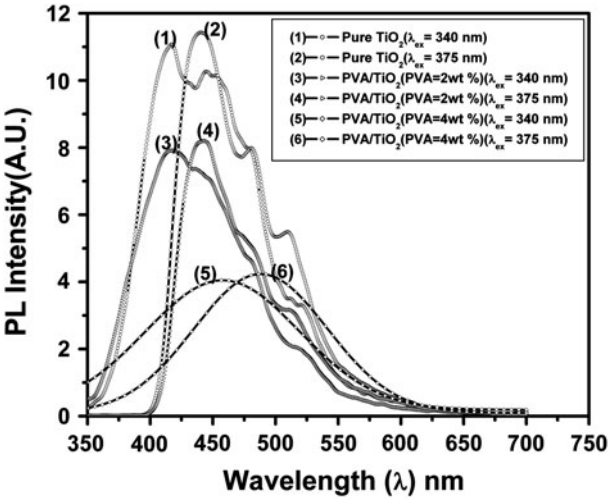

Fig. 9 Photoluminescence Spectra of pure TiO_2 and PVA (2 and 4 wt%)/TiO_2 nanocomposites at room temperature using 340 and 375 nm excitation line of xenon discharge lamp

Conclusion

From above discussion, we conclude that addition of small amount of PVA in TiO_2 increases its crystallinity. Also, we know that particle size as well as crystallinity increases with increase in temperature. But here we have seen that at only drying temperature of 35 °C (instead of 80 °C) in case of PVA/TiO_2 nanocomposites, we get larger particle size and high crystallinity in comparison to pure TiO_2. These effects occur due to PVA addition. TEM measurement showed the formation of nanorods which were highly dense. We increase the rod length and width of TiO_2 by doping it with PVA. Our studies revealed that by increasing the concentration of PVA in TiO_2 the band gap was lowered from 3.55 to 1.65 eV. Also, from the band gap analysis, we see that adding of PVA can make TiO_2 as a direct band gap semiconductor instead of indirect one. PL measurement suggested that addition of PVA in TiO_2 causes a reduction in impurity related centres and further increasing the amount of PVA can assist the emission towards visible region. In addition, since for the composite samples direct transitions dominate over indirect one, i.e., the nature of PVA/TiO_2 nanocomposite goes towards direct one so the sample can be useful for applications such as polymeric light emitting diodes, remote plasma treatment and large area flat panel display devices.

Acknowledgments Authors thankfully acknowledge Prof. Avinash C. Pandey and Prof R. Gopal for extending the facilities available with them at Nanotechnology Application Centre and Laser Spectroscopy Lab, Department of Physics, University of Allahabad, Allahabad, India, respectively. The UGC is also acknowledged for granting scholarship to Ms Archana Maurya.

References

1. Schnitzler DC, Meruvia MS, Hummelgen IA, Zarbin AJG (2003) Preparation and characterization of novel hybrid materials formed from (Ti, Sn)O_2 nanoparticles and polyaniline. Chem Mater 15:4658–4665
2. Chen GZ, Shaffer MSP, Coleby D, Dixon G, Zhou W, Fray DJ, Windle AH (2000) Carbon nanotube and polypyrrole composites: coating and doping. Adv Mater 12(7):522–526
3. Simonian AL, Good TA, Wang S-S, Wild JR (2005) Nanoparticle-based optical biosensors for the direct detection of organophosphate chemical warfare agents and pesticides. Anal Chim Acta 534:69–77
4. Justin Gooding J (2006) Biosensor technology for detecting biological warfare agents: recent progress and future trends. Anal Chim Acta 559:137–151
5. Wood A, Giersig M, Mulvaney P (2001) Fermi level equilibration in quantum dot−metal nanojunctions. J Phys Chem B 105:8810
6. O' Regan B, Grätzel M (1991) A low-cost, high-efficiency solar cell based on dye-sensitized colloidal TiO_2 films. Nature 353(1991):737–740
7. Tada H, Ishida T, Takao A, Ito S (2004) Synthesis, properties, and applications of oxide nanomaterials. Langmuir 20:7898
8. Zhang L-S, WU W-Z, WANG J-L (2007) Immobilization of activated sludge using improved polyvinyl alcohol (PVA) gel. J Environ Sci 19:1293–1297
9. Yang Dongzhi, Yanning Li, Nie Jun (2007) Preparation of gelatin/PVA nanofibers and their potential application in controlled release of drugs. Carbohydr Polym 69:538–543
10. Balaji Bhargav P, Madhu Mohan V, Sharma AK, Rao VVRN (2009) Investigations on electrical properties of (PVA:NaF) polymer electrolytes for electrochemical cell applications. Curr Appl Phys 9:165–171

11. Yang C-C (2007) Synthesis and characterization of the cross-linked PVA/TiO_2composite polymer membrane for alkaline DMFC. J Membr Sci 288:51–60
12. Sairam M, Patil MB, Veerapur RS, Patil SA, Aminabhavi TM (2006) Novel dense poly(vinyl alcohol)–TiO_2 mixed matrix membranes for pervaporation separation of water–isopropanol mixtures at 30 °C. J Membr Sci 281:95–102
13. Wang Z, Yamada S, Zhang M, Kanzaki H, Yoshinaga K (2010) Controlled crystallization of titanium dioxide particles in the presence of poly(vinyl alcohol) from peroxytitanic acid. Colloid Polym Sci 288:433–438
14. Bradlxey DC, Mehrotra RC, Gaur DP (1978) Metal alkoxides. Academic Press, New York, p 150
15. Meng L, Andritschky M, Santos M (1993) The effect of substrate temperature on the properties of DC reactive magnetron sputtered titanium oxide films. Thin Solid Films 223:242–247
16. Kumar PM, Badrinarayanan S, Sastry M (2000) Nanocrystalline TiO_2 studied by optical, FTIR and X-ray photoelectron spectroscopy: correlation to presence of surface stress. Thin Solid Films 358:122
17. Mardare D, Tasca M, Delibas M, Rusu GI (2000) On the structural properties and optical transmittance of TiO_2 sputtered thin films. Appl Surf Sci 156:200–206
18. Gratzel M (1989) Heterogeneous photochemical electron transfer. CRC Press, Inc, Boca Raton